

A new method for computing the quark-gluon vertex

A. C. Aguilar

University of Campinas - UNICAMP, Institute of Physics “Gleb Wataghin”,
CEP 13083-859 - Campinas, SP, Brazil

E-mail: aguilar@ifi.unicamp.br

Abstract.

In this talk we present a new method for determining the nonperturbative quark-gluon vertex, which constitutes a crucial ingredient for a variety of theoretical and phenomenological studies. This new method relies heavily on the exact all-order relation connecting the conventional quark-gluon vertex with the corresponding vertex of the background field method, which is Abelian-like. The longitudinal part of this latter quantity is fixed using the standard gauge technique, whereas the transverse is estimated with the help of the so-called transverse Ward identities. This method allows the approximate determination of the nonperturbative behavior of all twelve form factors comprising the quark-gluon vertex, for arbitrary values of the momenta. Numerical results are presented for the form factors in three special kinematical configurations (soft gluon and quark symmetric limit, zero quark momentum), and compared with the corresponding lattice data.

1. Introduction

One of the major challenges of nonperturbative QCD is to understand the mechanism that drives chiral symmetry breaking and the associated generation of constituent quark masses. As is well known from a series of previous studies [1, 2, 3, 4, 5], the quantity that is intimately related to the underlying dynamics of the chiral symmetry breaking is the *quark-gluon vertex*. In addition, this vertex is of paramount importance in the formalism of the Bethe-Salpeter equations (BSEs), which describes the formation of the bound states of the theory [6, 7, 8, 9, 10, 11].

From the point of view of the perturbative QCD, the quark-gluon vertex has been carefully scrutinized at the one-loop level [12], where results for general kinematic configurations and arbitrary gauges. Moreover, at two and three-loop order we have results for some specific kinematics and gauges [13, 14].

The main difficulty in dealing with the quark-gluon vertex lies in the fact that one has to determine the behavior of twelve form factors (four “longitudinal” and the eight “transverse”), which are functions of three independent kinematic variables. For this reason, the available nonperturbative information on this quantity is rather limited. In particular, there are only few results obtained from simulations on relatively small lattices [15, 16, 17, 18, 19, 20]. In the context of the Schwinger-Dyson equations (SDEs) the situation is not that different. The behavior of the form factors is governed by a complex system of coupled integral equations, which can be solved only after considerable truncations and drastic simplifying assumptions [21, 22, 11, 23, 24, 25, 26].

In this talk we will present a novel nonperturbative approach for calculating the form factors of the quark-gluon vertex in the Landau gauge [27]. This task will be accomplished within the PT-BFM scheme [28, 29, 30], which is obtained from the combination of the pinch technique (PT) [31, 32, 33, 34, 35, 36] with the background field method (BFM) [37].

An intrinsic feature of the PT-BFM formalism is the natural separation of the gluonic field into a quantum and a background part, thus increasing the number of possible Green's functions that one may consider. In particular, two types of the quark-gluon vertices make their appearance: (i) the conventional quark-gluon vertex (formed by a quantum gluon, quark and anti-quark fields), denoted by Γ ; and the background quark-gluon vertex (formed by a background gluon, quark and anti-quark fields), denoted by $\widehat{\Gamma}$. A crucial difference between these two vertices, lies in the fact that the conventional vertex satisfies the usual STIs, whereas the background vertex obeys Abelian-like WIs. The conversion between quantum and background vertices is achieved through the so-called background-quantum identities (BQIs) [38, 39], which relate Γ and $\widehat{\Gamma}$ through special auxiliary ghost Green's functions, namely $\Lambda_{\mu\nu}$, K_μ and its conjugated \overline{K}_μ .

The aim of this work is to express the conventional quark-gluon vertex as a deviation from the ‘‘Abelian-like’’ vertex $\widehat{\Gamma}_\mu$. Specifically, our strategy will be the following: first we use the ‘‘gauge technique’’ inspired Ansatz [40, 41, 42, 43] for the longitudinal part of the Abelian-like $\widehat{\Gamma}_\mu$. Then, with the help of the so-called ‘‘Transverse Ward Identities’’ (TWIs) [44, 45, 46, 47, 48], we will fix the transverse part of the $\widehat{\Gamma}_\mu$, neglecting the non-local terms present in the TWIs. The combination of these two steps generates the so-called minimal Ansatz for $\widehat{\Gamma}_\mu$ [49]. As a final step we use the BQIs to convert $\widehat{\Gamma}_\mu$ into Γ . This conversion requires the computation of the special auxiliary functions $\Lambda_{\mu\nu}$ and K_μ ; the behavior of $\Lambda_{\mu\nu}$ is well-known from previous studies [50], whereas K_μ and \overline{K}_μ were first computed at one-loop dressed approximation in Ref. [27], using as ingredient the gluon lattice propagator.

In order to make contact with the results of lattice simulations [15, 16, 17, 18, 19, 20], we will present the numerical evaluation of the relevant form factors in three special kinematical configurations namely (i) soft gluon, (ii) quark symmetric limit and (iii) zero quark momentum. As we will see, while a general qualitative agreement with the available lattice data is found, quantitative discrepancies still remain.

2. The two quark-gluon vertices in the PT-BFM formalism

In the PT-BFM formalism there are two quark-gluon vertices, depending on the nature of the incoming gluon. Specifically, the vertex formed by a quantum gluon (Q) entering into a $\psi\bar{\psi}$ pair corresponds to the conventional vertex, Γ_μ^a (see left vertex of Fig. 1); the corresponding three-point function with a background gluon (\widehat{A}) entering represents instead the PT-BFM vertex, and will be denoted by $\widehat{\Gamma}_\mu^a$ (see right vertex of Fig. 1). Choosing the flow of the momenta such that $p_1 = q + p_2$, we then define

$$i\Gamma_\mu^a(q, p_2, -p_1) = igt^a\Gamma_\mu(q, p_2, -p_1); \quad i\widehat{\Gamma}_\mu^a(q, p_2, -p_1) = igt^a\widehat{\Gamma}_\mu(q, p_2, -p_1), \quad (1)$$

where the hermitian and traceless generators t^a of the fundamental SU(3) representation are given by $t^a = \lambda^a/2$, with λ^a the Gell-Mann matrices.

It is important to stress that Γ_μ and $\widehat{\Gamma}_\mu$ coincide only at tree-level, where one has $\Gamma_\mu^{(0)} = \widehat{\Gamma}_\mu^{(0)} = \gamma_\mu$.

The essential difference between these two vertices is that $\widehat{\Gamma}_\mu$ obeys the QED-like WI [37]

$$q^\mu\widehat{\Gamma}_\mu(q, p_2, -p_1) = S^{-1}(p_1) - S^{-1}(p_2), \quad (2)$$

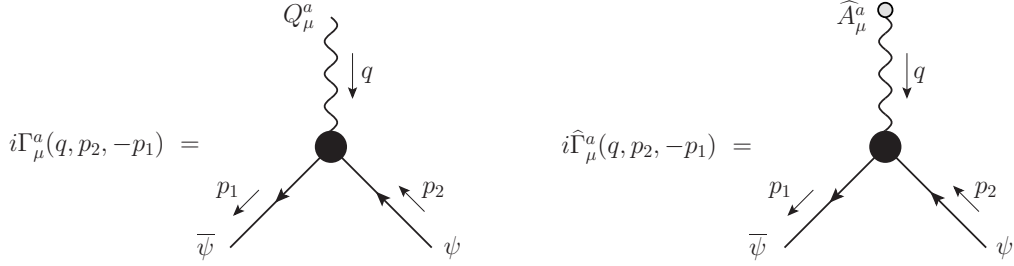


Figure 1. The conventional and background quark-gluon vertex with the momenta routing used throughout the text.

instead of the standard STI

$$q^\mu \Gamma_\mu(q, p_2, -p_1) = F(q^2) [S^{-1}(p_1)H(q, p_2, -p_1) - \overline{H}(-q, p_1, -p_2)S^{-1}(p_2)], \quad (3)$$

satisfied by Γ_μ . In both expressions, $S^{-1}(p) = A(p^2)\not{p} - B(p^2)$, is the inverse of the full quark propagator, defined in terms of the wave function, $A(p^2)$, and the mass function $B(p^2)$. In addition, $F(q^2)$ denotes the ghost dressing function, related to the full ghost propagator by $D(q^2) = F(q^2)/q^2$, whereas the functions $H^a = -gt^a H$ and its conjugated $\overline{H}^a = gt^a \overline{H}$ correspond to the so-called quark-ghost kernel, and are shown in Fig. 2.

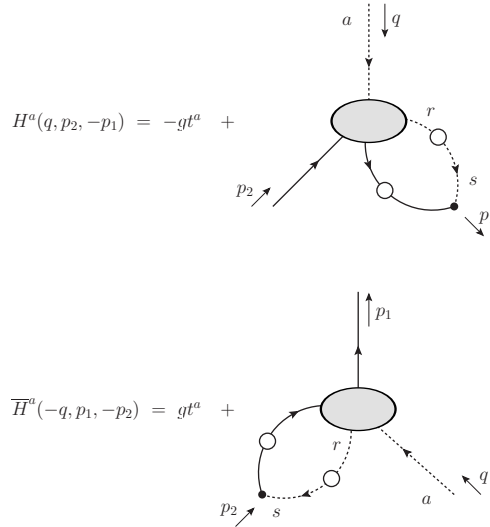


Figure 2. The ghost kernels H and \overline{H} appearing in the STI satisfied by the quark vertex Γ_μ . The composite operators ψc^s and $\overline{\psi} c^s$ have the tree-level expressions $-gt^a$ and gt^a respectively.

Notice that the quark-ghost kernel admits the general decomposition [12]

$$\begin{aligned} H(q, p_2, -p_1) &= X_0 \mathbb{I} + X_1 \not{p}_1 + X_2 \not{p}_2 + X_3 \tilde{\sigma}_{\mu\nu} p_1^\mu p_2^\nu, \\ \overline{H}(-q, p_1, -p_2) &= \overline{X}_0 \mathbb{I} + \overline{X}_2 \not{p}_1 + \overline{X}_1 \not{p}_2 + \overline{X}_3 \tilde{\sigma}_{\mu\nu} p_1^\mu p_2^\nu, \end{aligned} \quad (4)$$

where $\tilde{\sigma}_{\mu\nu} = \frac{1}{2}[\gamma_\mu, \gamma_\nu]$ and we have introduced the compact notation on the form factors $X_i = X_i(q^2, p_2^2, p_1^2)$ and $\overline{X}_i = X_i(q^2, p_1^2, p_2^2)$. Notice that at tree-level, one clearly has $X_0^{(0)} = \overline{X}_0^{(0)} = 1$, with the remaining form factors vanishing.

It is important to stress here that a set of identities, called background quantum identities (BQIs) [38, 39], relate the conventional and PT-BFM vertices. The BQI of interest in our case reads [30]

$$\begin{aligned} \widehat{\Gamma}_\mu(q, p_2, -p_1) &= \left[g_\mu^\nu (1 + G(q^2)) + \frac{q_\mu q^\nu}{q^2} L(q^2) \right] \Gamma_\nu(q, p_2, -p_1) \\ &\quad - S^{-1}(p_1) K_\mu(q, p_2, -p_1) - \overline{K}_\mu(-q, p_1, -p_2) S^{-1}(p_2), \end{aligned} \quad (5)$$

where, in the Landau gauge, the special functions K_μ and its conjugated \overline{K}_μ are related to the quark-ghost kernel H (and its conjugated) in the following way

$$\begin{aligned} H(q, p_2, -p_1) &= 1 + q^\mu K_\mu(q, p_2, -p_1), \\ \overline{H}(-q, p_1, -p_2) &= 1 - q^\mu \overline{K}_\mu(-q, p_1, -p_2). \end{aligned} \quad (6)$$

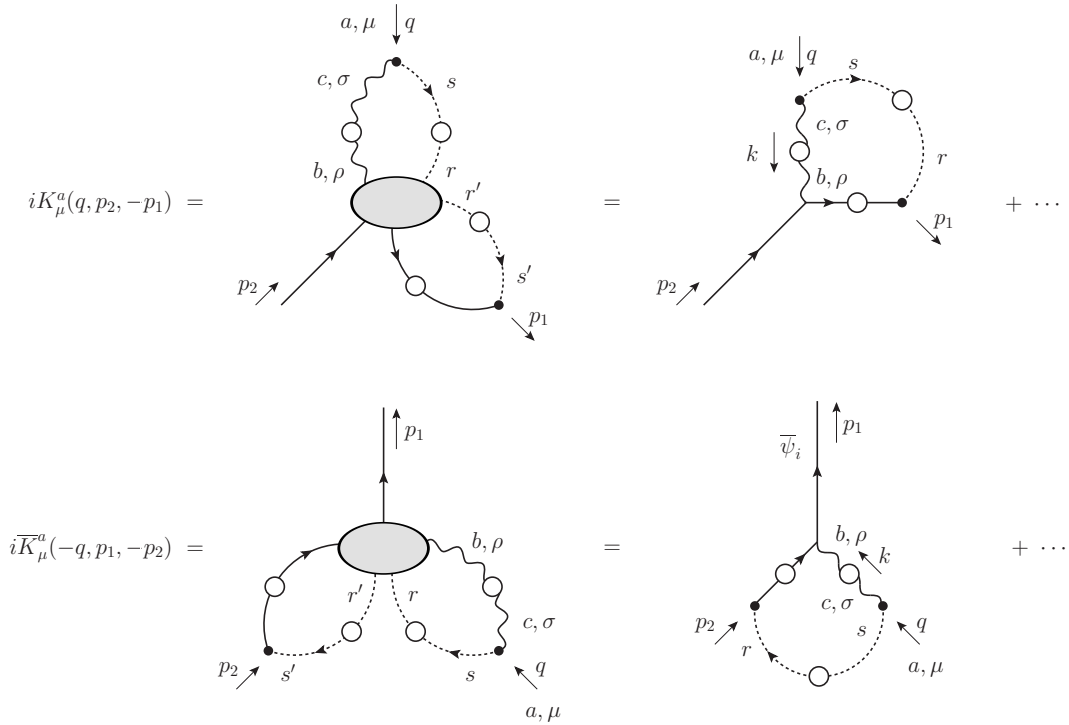


Figure 3. The auxiliary functions K_μ and \overline{K}_μ appearing in the BQI relating the conventional quark vertex Γ_μ with the PT-BFM vertex $\widehat{\Gamma}_\mu$. The diagrams on the right represent the one-loop dressed approximation of the two functions.

In what follows we will use the one-loop dressed approximation, in which the propagators are fully dressed while vertices are retained at their tree-level (see Fig. 3 again). This approximation yields the following expressions

$$\begin{aligned} K_\mu(q, p_2, -p_1) &= \frac{i}{2} g^2 C_A \int_k S(k + p_2) \gamma^\nu P_{\mu\nu}(k) \Delta(k^2) D(k - q), \\ \overline{K}_\mu(-q, p_1, -p_2) &= \frac{i}{2} g^2 C_A \int_k \gamma^\nu S(p_1 - k) P_{\mu\nu}(k) \Delta(k^2) D(k - q), \end{aligned} \quad (7)$$

The figure shows two equations with diagrams. The first equation is $\Lambda_{\mu\nu}(q) =$ followed by a diagram of a ghost loop (dashed line with two vertices) plus a diagram of a ghost loop with a gluon loop (solid line with two vertices) attached to one of the ghost vertices. The second equation is $H_{\nu\mu}(q, p, r) = g_{\mu\nu} +$ followed by a diagram of a ghost loop with a gluon loop attached to one vertex. The gluon loop has external momenta r and q , and the ghost loop has external momenta μ and ν .

Figure 4. The auxiliary function $\Lambda_{\mu\nu}$ appearing in the BQI relating the conventional quark vertex Γ_μ with the PT-BFM vertex $\widehat{\Gamma}_\mu$. The diagrammatic representation of the gluon-ghost scattering kernel $H_{\mu\nu}$.

where C_A represents the Casimir eigenvalue of the adjoint representation [$C_A = N$ for $SU(N)$], $d = 4 - \epsilon$ is the space-time dimension, and we have introduced the integral measure $\int_k = \mu^\epsilon \int d^d k / (2\pi)^d$, with μ the 't Hooft mass.

The functions $G(q^2)$ and $L(q^2)$ appearing in Eq. (5) are the tensorial projections of the special two-point function

$$\begin{aligned} \Lambda_{\mu\nu}(q) &= -ig^2 C_A \int_k \Delta_\mu^\sigma(k) D(q-k) H_{\nu\sigma}(-q, q-k, k) \\ &\equiv g_{\mu\nu} G(q^2) + \frac{q_\mu q_\nu}{q^2} L(q^2), \end{aligned} \quad (8)$$

Finally, $H_{\mu\nu}$ is the ghost-gluon scattering kernel, and $\Delta_{\mu\nu}(q)$ is the gluon propagator defined in the Landau gauge as

$$i\Delta_{\mu\nu}(q) = -iP_{\mu\nu}(q)\Delta(q^2), \quad P_{\mu\nu}(q) = g_{\mu\nu} - q_\mu q_\nu / q^2. \quad (9)$$

Interestingly enough, in the Landau gauge the form factors $G(q^2)$ and $L(q^2)$ are related to the ghost dressing function $F(q^2)$ by the all-order relation [51, 50]

$$F^{-1}(q^2) = 1 + G(q^2) + L(q^2). \quad (10)$$

The most general tensorial decomposition of the quark-gluon vertex contains four longitudinal and eight transverse form factors. Using transverse and longitudinal (T+L) basis [12, 52], we can write

$$\Gamma^\mu(q, p_2, -p_1) = \sum_{i=1}^4 \Gamma_i^L(q^2, p_2^2, p_1^2) L_i^\mu(q, p_2, -p_1) + \sum_{i=1}^8 \Gamma_i^T(q^2, p_2^2, p_1^2) T_i^\mu(q, p_2, -p_1), \quad (11)$$

where the longitudinal basis vectors read (remember that $t = p_1 + p_2$)

$$L_1^\mu = \gamma^\mu; \quad L_2^\mu = \not{t} t^\mu; \quad L_3^\mu = t^\mu; \quad L_4^\mu = \tilde{\sigma}^{\mu\nu} t_\nu; \quad (12)$$

while for the transverse basis vectors we have instead

$$\begin{aligned}
T_1^\mu &= p_2^\mu(p_1 \cdot q) - p_1^\mu(p_2 \cdot q); & T_2^\mu &= T_1^\mu \not{t}; \\
T_3^\mu &= q^2 \gamma^\mu - q^\mu \not{q}; & T_4^\mu &= T_1^\mu \tilde{\sigma}_{\nu\lambda} p_1^\nu p_2^\lambda; \\
T_5^\mu &= \tilde{\sigma}^{\mu\nu} q_\nu; & T_6^\mu &= \gamma^\mu(q \cdot t) - t^\mu \not{q}; \\
T_7^\mu &= -\frac{1}{2}(q \cdot t)L_4^\mu - t^\mu \tilde{\sigma}_{\nu\lambda} p_1^\nu p_2^\lambda; & T_8^\mu &= \gamma^\mu \tilde{\sigma}_{\nu\lambda} p_1^\nu p_2^\lambda + p_2^\mu \not{p}_1 - p_1^\mu \not{p}_2.
\end{aligned} \tag{13}$$

In addition to the usual WI (2) and STI (3), specifying the *divergence* of the quark-gluon vertex $\partial^\mu \Gamma_\mu$, there exists a set of less familiar identities, called transverse Ward identities (TWIs) [44, 45, 46, 47, 48, 49], which give information on the *curl* of the vertex, $\partial_\mu \Gamma_\nu - \partial_\nu \Gamma_\mu$.

In the case of an Abelian gauge theory, one may consider a fermion coupling to a gauge boson through a vector vertex Γ_μ and an axial-vector vertex Γ_μ^A . In this case the TWIs read [49]

$$\begin{aligned}
q_\mu \Gamma_\nu(q, p_2, -p_1) - q_\nu \Gamma_\mu(q, p_2, -p_1) &= i[S^{-1}(p_2)\tilde{\sigma}_{\mu\nu} - \tilde{\sigma}_{\mu\nu}S^{-1}(p_1)] + 2im\Gamma_{\mu\nu}(q, p_2, -p_1) \\
&\quad + t^\lambda \epsilon_{\lambda\mu\nu\rho} \Gamma_\lambda^\rho(q, p_2, -p_1) + A_{\mu\nu}^V(q, p_2, -p_1), \\
q_\mu \Gamma_\nu^A(q, p_2, -p_1) - q_\nu \Gamma_\mu^A(q, p_2, -p_1) &= i[S^{-1}(p_2)\tilde{\sigma}_{\mu\nu}^5 - \tilde{\sigma}_{\mu\nu}^5 S^{-1}(p_1)] \\
&\quad + t^\lambda \epsilon_{\lambda\mu\nu\rho} \Gamma_\lambda^\rho(q, p_2, -p_1) + V_{\mu\nu}^A(q, p_2, -p_1),
\end{aligned} \tag{14}$$

where $\tilde{\sigma}_{\mu\nu}^5 = \gamma_5 \tilde{\sigma}_{\mu\nu}$, $\epsilon_{\lambda\mu\nu\rho}$ is the totally antisymmetric Levi-Civita tensor, while $\Gamma_{\mu\nu}$, $A_{\mu\nu}^V$, and $V_{\mu\nu}^A$ represent non-local tensor vertices that appear in this type of identities.

As was shown in Ref. [49], it is possible to disentangle the vector and the axial-vector vertices appearing in Eq. (14). Specifically, for the vector vertex we obtain

$$[t^\mu \theta_\mu^i q_\rho - (q \cdot t) \theta_\rho^i] \Gamma^\rho(q, p_2, -p_1) = P_i^{\mu\nu} \{i[S^{-1}(p_2)\tilde{\sigma}_{\mu\nu}^5 - \tilde{\sigma}_{\mu\nu}^5 S^{-1}(p_1)] + V_{\mu\nu}^A(q, p_2, -p_1)\}, \tag{15}$$

where the tensorial projectors are defined as

$$P_i^{\mu\nu} = \frac{1}{2} \epsilon^{\alpha\mu\nu\beta} \theta_\alpha^i q_\beta, \quad i = 1, 2; \quad \theta_\alpha^1 = t_\alpha, \quad \theta_\alpha^2 = \gamma_\alpha. \tag{16}$$

In what follows we will use Eq. (15) in conjunction with the WI (2) in order to determine the complete set of form factors characterizing the vertex $\hat{\Gamma}_\mu$. After that, we will apply the BQI given by Eq. (5) to obtain the final expression for Γ_μ .

3. Special kinematic configurations

In this section, we will present the results for three special kinematic configurations: (i) the soft gluon limit, (ii) the symmetric limit and (iii) the zero quark momenta configuration. The general expressions, which are valid a generic configuration, can be found in Ref. [27].

3.1. Soft-gluon limit

Let us start with the soft limit, obtained when we take the limit of $p_1 \rightarrow p_2$ or similarly $q \rightarrow 0$. In this limit all the transverse tensor structures (13) vanish identically. The vertex is therefore purely longitudinal, and after setting $p_1 = p_2 = p$, the longitudinal tensorial structures reduce ($p_1 = p_2 = p$) to

$$L_1^\mu = \gamma^\mu; \quad L_2^\mu = 4\not{p}p^\mu; \quad L_3^\mu = 2p^\mu; \quad L_4^\mu = 2\tilde{\sigma}^{\mu\nu} p_\nu. \tag{17}$$

The form factors that accompany each one of the above tensorial structures are given by

$$\begin{aligned}
F_0^{-1}\Gamma 1 &= A(1 - 2p^2 K_4) - 2BK_1, \\
F_0^{-1}\Gamma 2 &= 2A' + 2A(K_3 + K_4) - 2BK_2, \\
F_0^{-1}\Gamma 3 &= -2B' + 2A(K_1 + p^2 K_2) - 2BK_3, \\
\Gamma 4 &= 0,
\end{aligned}
\tag{18}$$

where $F_0^{-1} = F^{-1}(0)$, $A = A(p^2)$, $B = B(p^2)$, $K_i = K_i(p^2)$, and a prime denotes the derivative with respect to p^2 . The K_i correspond to the decomposition of the tensorial structure of Eq. (7) in the basis presented in Eq. (11), and its detailed derivation is given in Ref. [27].

All ingredients that are necessary for computing the $K_i = K_i(p^2)$ are renormalized at $\mu = 2.0$ GeV. In particular, we use the SU(3) gluon propagator, $\Delta(q)$, obtained by the lattice simulation of Ref. [53], the solution of the SDE for ghost dressing function, $F(q)$, and the auxiliary functions $1 + G(q)$ and $L(q)$. All these quantities were computed using $\alpha(\mu) = 0.45$. In addition, the behavior of the functions $A(p)$ and $B(p)$ were obtained by solving the quark gap equation for a current mass $m_0 = 115$ MeV.

In Fig. 5 we plot the functions K_i in the soft gluon limit. With the K_i at hand, the next step is to determine the vertex form factors of Eq. (18).

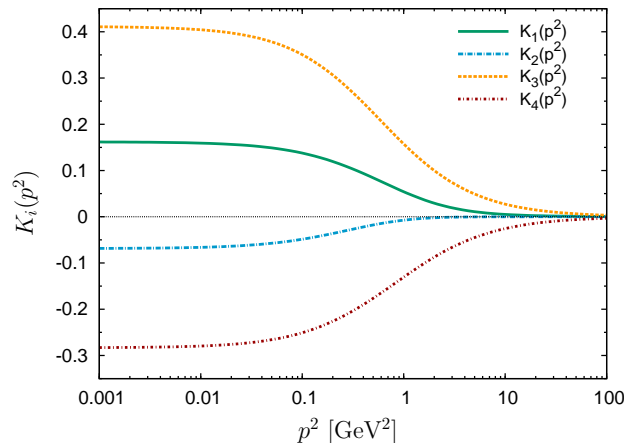


Figure 5. (color online). The auxiliary functions K_i evaluated in the soft gluon limit.

Specifically, in Figs. 6 and 7 we plot the form factors

$$\lambda_1(p) = \Gamma_1^E(p_E); \quad \lambda_2(p) = \frac{1}{4}\Gamma_2^E(p_E); \quad \lambda_3(p) = -\frac{1}{2}\Gamma_3^E(p_E),
\tag{19}$$

and compare them with the lattice data of [17], obtaining rather reasonable agreement.

3.2. Symmetric limit

The symmetric limit is defined taking $p_1 \rightarrow -p_2$. In this limit, only one longitudinal basis tensor (12) and two transverse tensors (13) survive. Specifically we have

$$L_1^\mu = \gamma^\mu; \quad T_3^\mu = 4(p^2 \gamma^\mu - p^\mu \not{p}); \quad T_5^\mu = -2\tilde{\sigma}^{\mu\nu} p_\nu.
\tag{20}$$

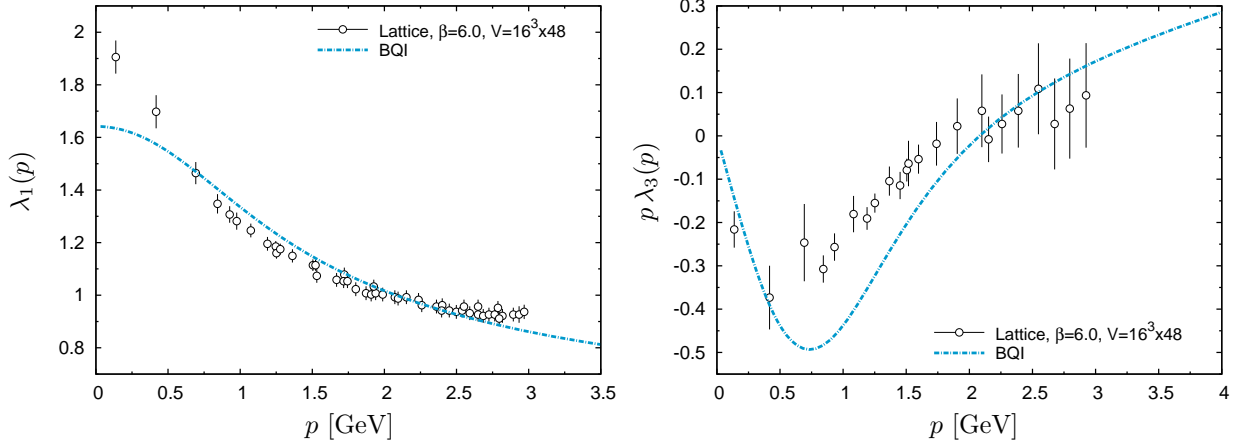


Figure 6. (color online). The soft gluon form factors λ_1 (left) and $p\lambda_3$ (right). Lattice data in this and all the following plots are taken from [17].

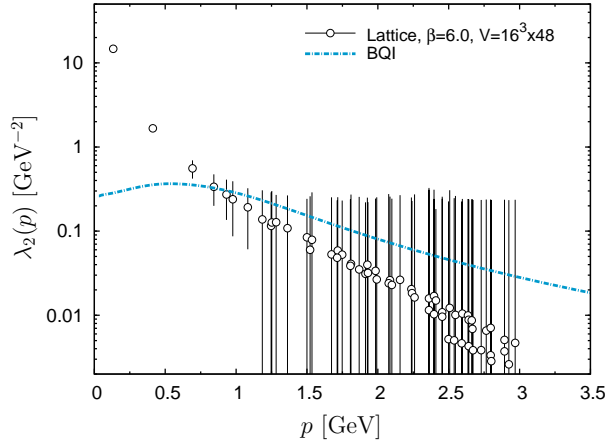


Figure 7. (color online). The form factor λ_2 and the corresponding lattice data.

However, the lattice simulations can not determine separately the form factors that accompanies the tensorial structures above described; only combinations of the type

$$\begin{aligned}\mathcal{G}_{2p}(\Gamma_1^L + p^2\Gamma_3^T) &= 2p^2A' + A(1 + 2p^2K_5^T) - 2B(K_1^L + p^2K_3^T), \\ \mathcal{G}_{2p}\Gamma_5^T &= 2B' + 2A(K_1^L + p^2K_3^T) - 2BK_5^T.\end{aligned}\quad (21)$$

can be extracted. In the above equation the compact notation $A = A(p^2)$, $B = B(p^2)$ and $\mathcal{G}_{2p} = 1 + G(4p^2)$ has been introduced.

Using the same ingredients described in the soft gluon case, we have computed the corresponding K_i for the symmetric configuration, which are presented in Fig. 8. In this limit, we clearly see that we have a divergent K_2 and a finite K_4 .

The next step is to compare our numerical results for the Euclidean version of the form factors combinations of Eq. (21) with the lattice data of Ref. [17]. This comparison is shown in Fig. 9, where we have defined

$$\lambda_1'(p) = \Gamma_1^{LE}(p_E) - p_E^2\Gamma_3^{TE}(p_E); \quad \tau_5(p) = \frac{1}{2}\Gamma_5^{TE}(p_E), \quad (22)$$

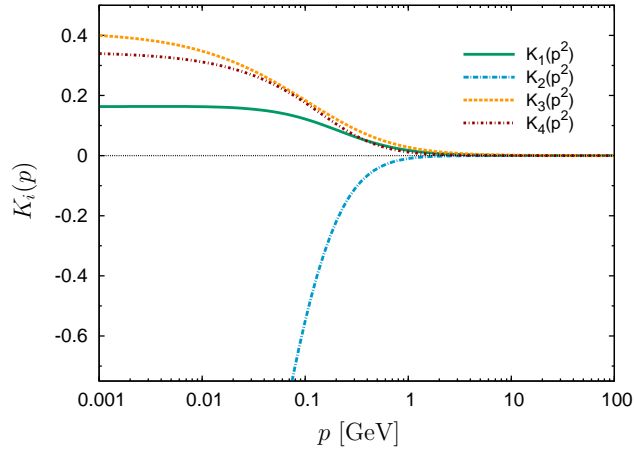


Figure 8. (color online). The auxiliary functions K_i evaluated in the symmetric gluon limit.

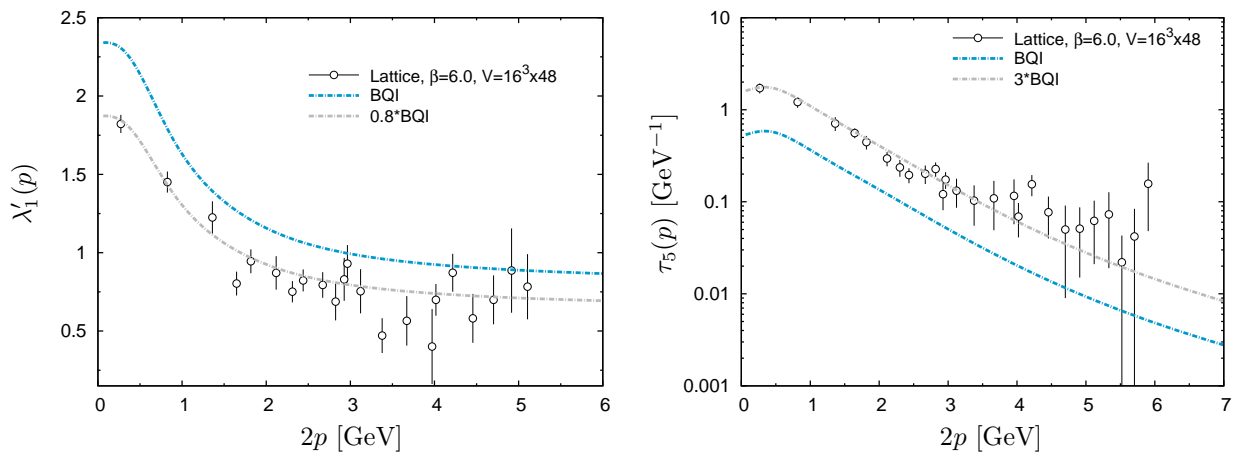


Figure 9. (color online). The symmetric limit form factors λ_1' and τ_5 compared with the corresponding lattice data. The grey curves are obtained through simple rescaling of the blue ones.

Clearly, we see that the overall shape of the both form factors are correctly reproduced; however, the overlap with the lattice data is only obtained if we rescale our results by (different) multiplicative factors, giving rise to the gray curves.

In Figs. 10 and 11 we plot, for completeness the three non-zero form factors separately. Notice that both Γ_1^L and Γ_5^T are finite, whereas Γ_3^T is divergent.

3.3. Zero quark momentum

The next limit that we will present here is the so-called zero quark configuration, where we set to zero the quark momentum p_2 , which leads to $q = p_1 = p$. A crucial difference of this case compared with the previous one is that the $K_i^{L,T}(p^2, 0, p^2)$ and $\overline{K}_i^{L,T}(p^2, p^2, 0)$ do not coincide anymore, and need to be evaluated separately. More specifically, the non-zero form factors are

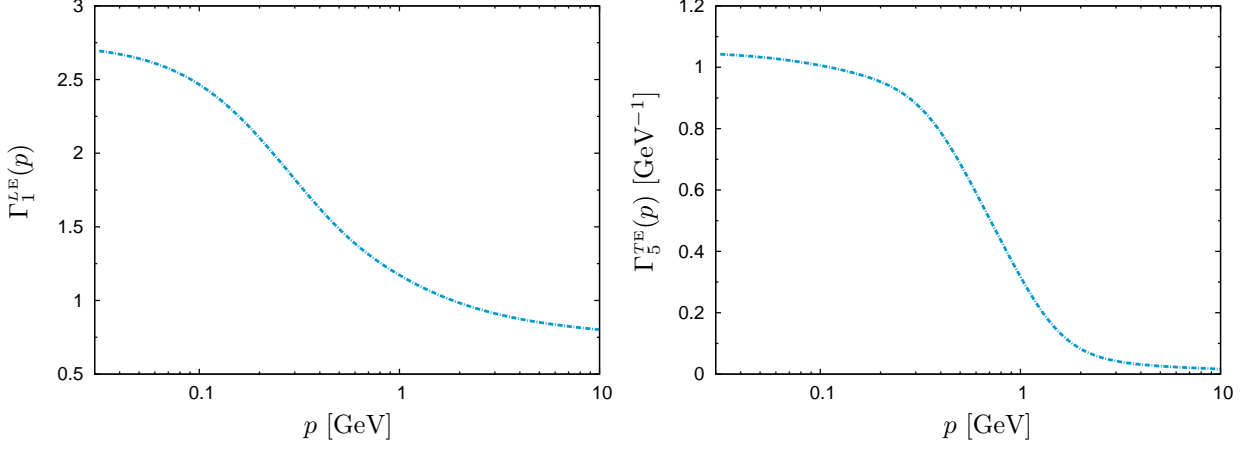


Figure 10. (color online). The symmetric form factors Γ_1^L (left) and Γ_5^T (right).

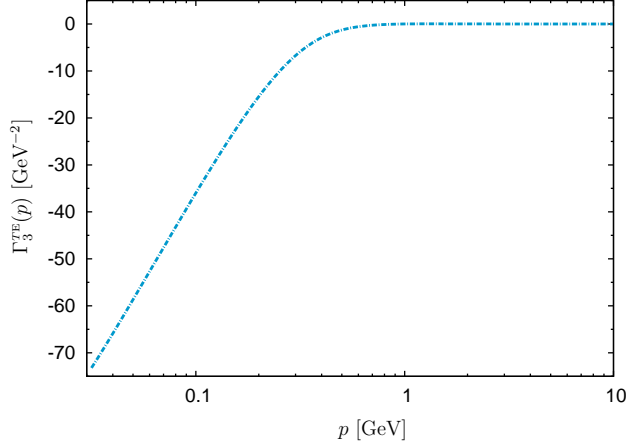


Figure 11. (color online). The divergent form factor Γ_3^T in the symmetric limit.

expressed as

$$\begin{aligned}
F^{-1}\Gamma_1^L &= A(1 + p^2 K_3^L) - BK_1^L - B_0 \overline{K}_1^L, \\
F^{-1}\Gamma_3^L &= -\frac{1}{p^2}(B - B_0) + AK_1^L - BK_3^L - B_0 \overline{K}_3^L, \\
\mathcal{G}\Gamma_3^T &= -A(K_3^L + K_5^T) - BK_3^T - B_0 \overline{K}_3^T + \frac{1}{p^2} L_p F_p \left[A(1 + p^2 K_3^L) - BK_1^L - B_0 \overline{K}_1^L \right], \\
\mathcal{G}\Gamma_5^T &= -\frac{1}{p^2}(B - B_0) - A(K_1^L + p^2 K_3^T) - BK_5^T - B_0 \overline{K}_5^T,
\end{aligned} \tag{23}$$

with the usual definitions $A = A(p^2)$, $B = B(p^2)$, as well as $B_0 = B(0)$.

In Fig. 12 we show the auxiliary functions K_i (left) and \overline{K}_i (right) evaluated in the zero quark momentum configuration. Notice that all K_i and \overline{K}_i are IR finite except for K_2 and \overline{K}_2 which are divergent.

In Fig. 13 we show the Euclidean version of the numerical results for the form factors appearing in Eq. (23). In particular, we see the appearance of a negative divergence in the form factor $\Gamma_3^{T,E}$.

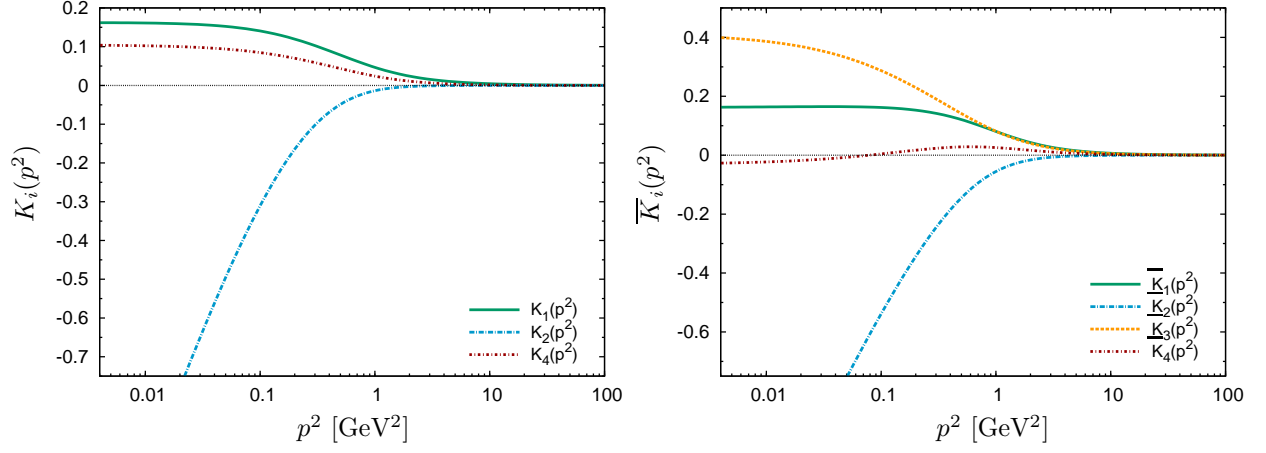


Figure 12. (color online). The auxiliary functions K_i (left) and \bar{K}_i (right) evaluated in the zero quark momentum configuration.

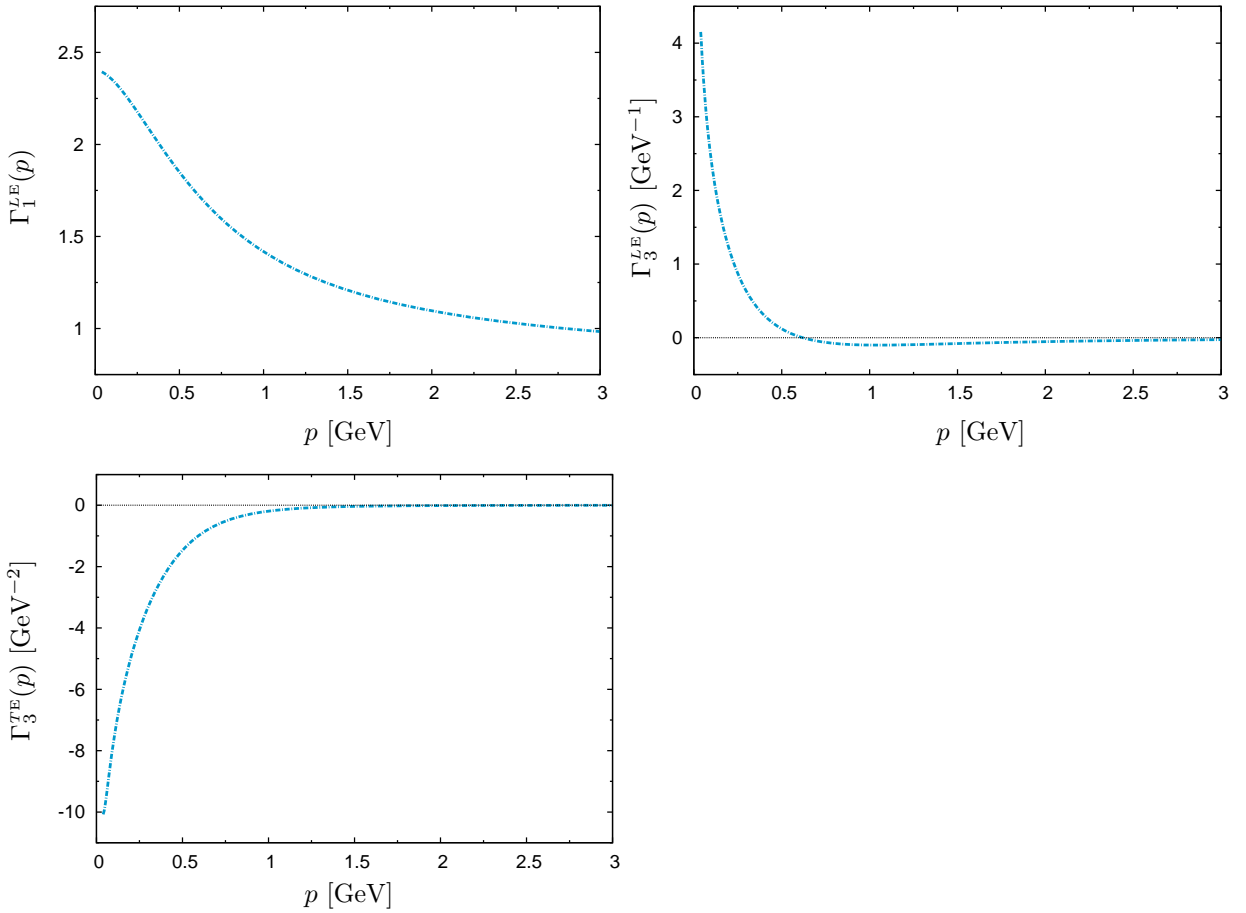


Figure 13. (color online). The form factors Γ_1^{LE} , Γ_3^{LE} and Γ_3^{TE} evaluated in the zero quark momentum configuration.

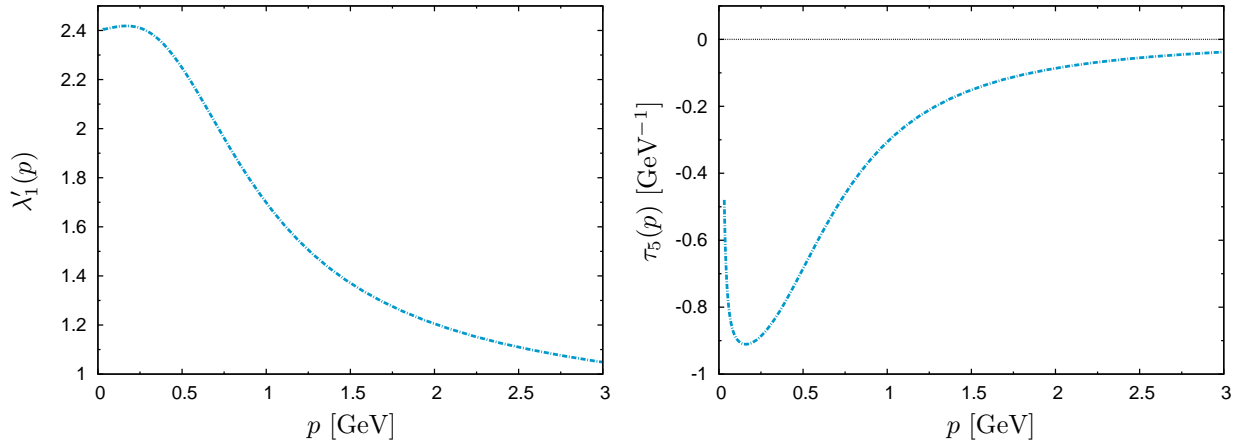


Figure 14. (color online). The form factors λ'_1 (left) and τ_5 (right) in the quark zero momentum configuration.

Although there is no lattice results for this kinematic limit, the combination that could be measured on the lattice would be of the type

$$\begin{aligned} \mathcal{G}(\Gamma_1^L + p^2\Gamma_3^T) &= A(1 - p^2K_5^T) - B(K_1^L + p^2K_3^T) - B_0(\overline{K}_1^L + p^2\overline{K}_3^T), \\ \mathcal{G}\Gamma_5^T &= -\frac{1}{p^2}(B - B_0) - A(K_1^L + p^2K_3^T) - BK_5^T - B_0\overline{K}_5^T. \end{aligned} \quad (24)$$

In this case, we present our “prediction” for these combinations in Fig. 14.

4. Conclusions

We have presented a new methodology for determining the longitudinal and transverse form factors of the nonperturbative quark-gluon vertex within the PT-BFM scheme. This scheme allows us to take the full advantage of the rich amount of information originating from the fundamental underlying symmetries, which are encoded in a set of crucial identities such as WIs, STIs and BQIs.

The key observation in this analysis is the connection between the two distinct quark-gluon vertices, Γ_μ and $\widehat{\Gamma}_\mu$, appearing in the PT-BFM scheme. Using the WIs and the TWIs satisfied by $\widehat{\Gamma}_\mu$, we first determine the form factors that describes the behavior of this Abelian-like type of vertex. Then, with the help of the BQI that connects both vertices, we obtain the final expression for the conventional Γ_μ .

We have shown that the BQI is expressed in terms of the auxiliary three-point functions K_μ , which were calculated in the one-loop dressed approximation. Already, at this level of approximation, we have obtained nontrivial information for all form-factors. In addition, we have noticed that the contributions originating from the K_i and \overline{K}_i are in general sizeable, and therefore the K_i and \overline{K}_i contribute significantly in obtaining results similar to those found in lattice simulations.

For the determination of the K_i and \overline{K}_i we have used as external ingredient the full gluon propagator, $\Delta(q^2)$, obtained in lattice simulations. The remaining necessary ingredients, namely the ghost dressing function $F(q^2)$ and the quark functions $A(p^2)$ and $B(p^2)$, were obtained solving numerically their corresponding SDEs.

For the purpose of this talk we have applied our formalism to three particular kinematic limits known as (i) “soft gluon”, (ii) “quark symmetric” and (ii) “zero quark momentum”

configurations, which give rise to considerable technical simplifications, especially in the calculation of the K_i and \bar{K}_i . Evidently, the numerical analysis presented here may be extended to arbitrary kinematic configurations, furnishing valuable information on such a fundamental quantity as the quark-gluon vertex, which constitutes a crucial ingredient for a variety of theoretical and phenomenological studies.

Acknowledgments

I would like to thank the organizers of the ‘‘Discrete 2014’’ for the pleasant conference and for the hospitality. The work of A. C. Aguilar is supported by the National Council for Scientific and Technological Development - CNPq under the grant 306537/2012-5 and project 473260/2012-3, and by Sao Paulo Research Foundation - FAPESP through the project 2012/15643-1.

References

- [1] Maris P and Roberts C D 2003 *Int.J.Mod.Phys.* **E12** 297–365 (*Preprint nucl-th/0301049*).
- [2] Roberts C D and Williams A G 1994 *Prog. Part. Nucl. Phys.* **33** 477–575 (*Preprint hep-ph/9403224*).
- [3] Fischer C S and Alkofer R 2003 *Phys.Rev.* **D67** 094020 (*Preprint hep-ph/0301094*).
- [4] Aguilar A C and Papavassiliou J 2011 *Phys.Rev.* **D83** 014013 (*Preprint 1010.5815*).
- [5] Cloet I C and Roberts C D 2014 *Prog. Part. Nucl. Phys.* **77** 1–69 (*Preprint 1310.2651*).
- [6] Maris P and Tandy P C 1999 *Phys. Rev.* **C60** 055214 (*Preprint nucl-th/9905056*).
- [7] Bender A, Detmold W, Roberts C and Thomas A W 2002 *Phys.Rev.* **C65** 065203 (*Preprint nucl-th/0202082*).
- [8] Bhagwat M, Holl A, Krassnigg A, Roberts C and Tandy P 2004 *Phys.Rev.* **C70** 035205 (*Preprint nucl-th/0403012*).
- [9] Holl A, Krassnigg A and Roberts C 2005 *Nucl.Phys.Proc.Suppl.* **141** 47–52 (*Preprint nucl-th/0408015*).
- [10] Chang L and Roberts C D 2009 *Phys. Rev. Lett.* **103** 081601 (*Preprint 0903.5461*).
- [11] Williams R 2014 (*Preprint 1404.2545*).
- [12] Davydychev A I, Osland P and Saks L 2001 *Phys. Rev.* **D63** 014022 (*Preprint hep-ph/0008171*).
- [13] Chetyrkin K and Seidensticker T 2000 *Phys.Lett.* **B495** 74–80 (*Preprint hep-ph/0008094*).
- [14] Chetyrkin K and Retey A 2000 (*Preprint hep-ph/0007088*).
- [15] Skullerud J, Bowman P O and Kizilersu A 2002 270–272 (*Preprint hep-lat/0212011*).
- [16] Skullerud J and Kizilersu A 2002 *JHEP* **0209** 013 (*Preprint hep-ph/0205318*).
- [17] Skullerud J I, Bowman P O, Kizilersu A, Leinweber D B and Williams A G 2003 *JHEP* **0304** 047 (*Preprint hep-ph/0303176*).
- [18] Skullerud J I, Bowman P O, Kizilersu A, Leinweber D B and Williams A G 2005 *Nucl.Phys.Proc.Suppl.* **141** 244–249 (*Preprint hep-lat/0408032*).
- [19] Lin H W 2006 *Phys.Rev.* **D73** 094511 (*Preprint hep-lat/0510110*).
- [20] Kizilersu A, Leinweber D B, Skullerud J I and Williams A G 2007 *Eur.Phys.J.* **C50** 871–875 (*Preprint hep-lat/0610078*).
- [21] Bhagwat M and Tandy P 2004 *Phys.Rev.* **D70** 094039 (*Preprint hep-ph/0407163*).
- [22] Llanes-Estrada F J, Fischer C S and Alkofer R 2006 *Nucl.Phys.Proc.Suppl.* **152** 43–46 (*Preprint hep-ph/0407332*).
- [23] Alkofer R, Fischer C S, Llanes-Estrada F J and Schwenzer K 2009 *Annals Phys.* **324** 106–172 (*Preprint 0804.3042*).
- [24] Matevosyan H H, Thomas A W and Tandy P C 2007 *Phys.Rev.* **C75** 045201 (*Preprint nucl-th/0605057*).
- [25] Aguilar A C, Binosi D, Cardona J and Papavassiliou J 2012 *PoS ConfinementX* 103 (*Preprint 1301.4057*).
- [26] Rojas E, de Melo J, El-Bennich B, Oliveira O and Frederico T 2013 *JHEP* **1310** 193 (*Preprint 1306.3022*).
- [27] Aguilar A C, Binosi D, Ibañez D and Papavassiliou J 2014 *Phys.Rev.* **D90** 065027 (*Preprint 1405.3506*).
- [28] Aguilar A C and Papavassiliou J 2006 *JHEP* **12** 012 (*Preprint hep-ph/0610040*).
- [29] Binosi D and Papavassiliou J 2008 *Phys.Rev.* **D77** 061702 (*Preprint 0712.2707*).
- [30] Binosi D and Papavassiliou J 2008 *JHEP* **0811** 063 (*Preprint 0805.3994*).
- [31] Cornwall J M 1982 *Phys. Rev.* **D26** 1453.
- [32] Cornwall J M and Papavassiliou J 1989 *Phys. Rev.* **D40** 3474.
- [33] Pilaftsis A 1997 *Nucl. Phys.* **B487** 467–491 (*Preprint hep-ph/9607451*).
- [34] Binosi D and Papavassiliou J 2002 *Phys. Rev.* **D66** 111901(R) (*Preprint hep-ph/0208189*).
- [35] Binosi D and Papavassiliou J 2004 *J.Phys.G* **G30** 203 (*Preprint hep-ph/0301096*).

- [36] Binosi D and Papavassiliou J 2009 *Phys. Rept.* **479** 1–152 (*Preprint* 0909.2536).
- [37] Abbott L F 1981 *Nucl. Phys.* **B185** 189.
- [38] Grassi P A, Hurth T and Steinhauser M 2001 *Annals Phys.* **288** 197–248 (*Preprint* hep-ph/9907426).
- [39] Binosi D and Papavassiliou J 2002 *Phys.Rev.* **D66** 025024 (*Preprint* hep-ph/0204128).
- [40] Salam A 1963 *Phys. Rev.* **130** 1287–1290.
- [41] Salam A and Delbourgo R 1964 *Phys. Rev.* **135** B1398–B1427.
- [42] Delbourgo R and West P C 1977 *J. Phys.* **A10** 1049.
- [43] Delbourgo R and West P C 1977 *Phys. Lett.* **B72** 96.
- [44] Takahashi Y 1985 *Canonical quantization and generalized Ward relations: Foundation of nonperturbative approach eralized Ward relations: Foundation of nonperturbative approach* (Print-85-0421 (Alberta)).
- [45] Kondo K I 1997 *Int.J.Mod.Phys.* **A12** 5651–5686 (*Preprint* hep-th/9608100).
- [46] He H X, Khanna F and Takahashi Y 2000 *Phys.Lett.* **B480** 222–228.
- [47] He H X 2006 *Commun.Theor.Phys.* **46** 109–112.
- [48] He H X 2007 *Int.J.Mod.Phys.* **A22** 2119–2132.
- [49] Qin S X, Chang L, Liu Y X, Roberts C D and Schmidt S M 2013 *Phys.Lett.* **B722** 384–388 (*Preprint* 1302.3276).
- [50] Aguilar A C, Binosi D and Papavassiliou J 2009 *JHEP* **0911** 066 (*Preprint* 0907.0153).
- [51] Grassi P A, Hurth T and Quadri A 2004 *Phys. Rev.* **D70** 105014 (*Preprint* hep-th/0405104).
- [52] Kizilersu A, Reenders M and Pennington M 1995 *Phys.Rev.* **D52** 1242–1259 (*Preprint* hep-ph/9503238).
- [53] Bogolubsky I, Ilgenfritz E, Muller-Preussker M and Sternbeck A 2009 *Phys. Lett.* **B676** 69–73 (*Preprint* 0901.0736).